CHAPTER 33

A Similarity Model in the Surf Zone

by

Hsiang Wang, Professor
Department of Civil Engineering and College of Marine Studies
University of Delaware
Newark, DE 19711

and

Wei-Chong Yang, Coastal Engineer
PRC Harris, Inc.
3003 New Hyde Park Road
Lake Success, NY 11042

1. INTRODUCTION

In fluid mechanics, a powerful tool known as the similarity model has been applied successfully to describe velocity and pressure fields in steady boundary layer flows, jet flows and wake flows. These flows, with the exception of a few laminar cases, are quite complex and are usually not amenable to theoretical analysis. The similarity analysis offers an alternative and often provides useful engineering information on the mean flow characteristics. The present work explores the possibility of applying the similarity concept to describe the flow field of breaking waves in the surf zone.

Before presenting the similarity solution, a non-dimensional surf zone parameter is examined. This parameter, in addition to its many implications of characterizing surf zone properties, is pertinent to defining the region of validity of the similarity solutions. Solutions on mean flow characteristics are then established based upon a similarity hypothesis which states that the profiles of flow properties such as velocity and wave form preserve geometrical similarity downstream from the source of the disturbance and, therefore, can be defined by a few local characteristic parameters. Conditions required to preserve similarity are examined. Finally, laboratory results from a number of studies (Flick, 1978; Svendsen et al., 1978; Sakai and Iwagaki, 1978) and those from the authors are used to test the validity of the proposed model.

2. SURF PARAMETER

Considering a single long-crested wave breaking on a beach of uniform slope, say tan α, the cyclic breaking process can be approximately divided into three stages as illustrated in Fig. 1. The developing stage covers the period when the wave begins incipient breaking at the crest until it collapses on the beach in the vicinity of the water level unit. During this stage, the shape of the wave evolves from a highly asymmetric curled form to a triangular form with numerous white caps. Its potential energy is converted into kinetic energy which in turn is partially dissipated as the remaining portion preserved to stage the upwash. In the second stage, the flow surges

up to its runup limit similar to a solid element moving up-slope while the kinetic energy is being converted back to potential energy. In the last stage, the flow washes down as a thin sheet to the breaking point to complete the cycle.

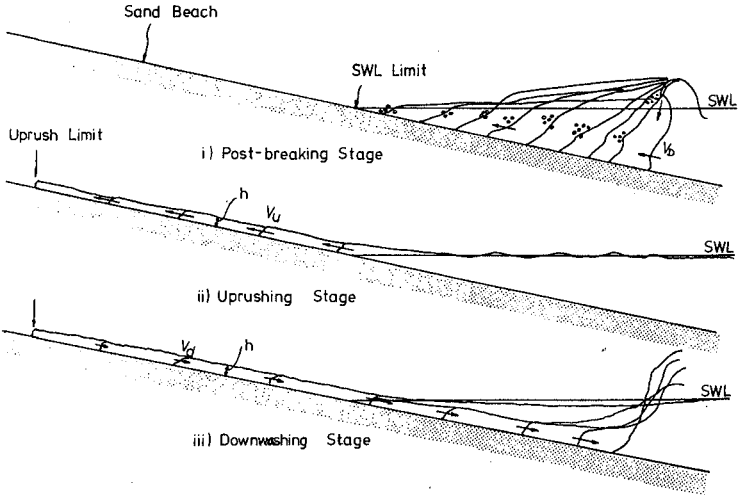

FIGURE 1. ILLUSTRATION OF BREAKING PROCESS.

The time required to complete each respective stage can be estimated based upon a simple energy model shown in Fig. 2. This energy

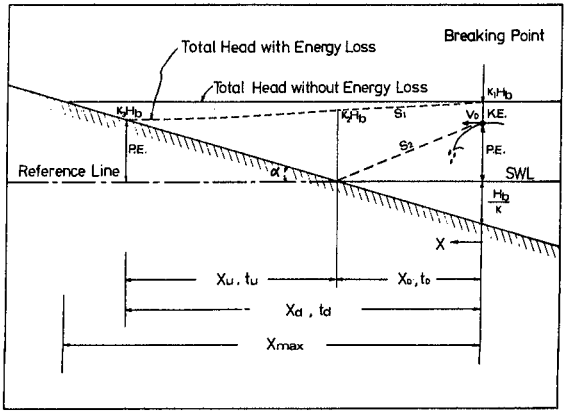

FIGURE 2. ENERGY CONSIDERATION OF BREAKING WAVE.

model is based upon the premise that the fluid element at the crest of the wave during breaking remains at the crest and is the same element that reaches the runup limit. This condition is clearly observed from recorded slow-motion films.

If the kinetic energy of the fluid element at the wave crest at the breaking point is assumed to be proportional to the breaking height, say $k_1 H_b$, then the kinetic energy in the developing stage can be expressed as

$$KE(x) = k_1 H_b + (S_2 - S_1)x \tag{1}$$

where S_2 and S_1 are the slopes of the total energy line and potential energy line, respectively. The velocity of the fluid element is

$$V_D(x) = \sqrt{2g[k_1 H_b + (S_2 - S_1)x]} \tag{2}$$

and the corresponding time required for the element travelling from the breaking point to the water level limit is

$$t_D = \int_0^{x_D} \frac{dx}{V_D(x)} = \frac{\sqrt{2}(\sqrt{k_2} - \sqrt{k_1})}{k(k_2 - k_1)} \frac{H_b^{1/2}}{g^{1/2} \tan \alpha} \tag{3}$$

where k_2 and k are constants of proportionality as defined in Fig. 2.

During the uprush and downwash stages, the crest element can be treated as a solid body moving on a sloped plan. In such cases, we have the following relationship on the basis of Newton's second law:

$$\mp Mg \sin \alpha - \rho f A_o \frac{V|V|}{8} = M \frac{dv}{dt} \tag{4}$$

where f is a frictional coefficient and A_o is the contact surface area; the "-" sign corresponds to the uprush condition and the "+" sign the downwash case. If we let $M = \rho t_h A_o$ the above equation simplifies to

$$\mp g \sin \alpha - \rho f \frac{V|V|}{8 t_h} = \frac{dv}{dt} \tag{5}$$

where t_h is the thickness of the runup water sheet. Equation (5) can be integrated to obtain the uprush and downwash time which are, respectively,

$$t_u = \left(2\sqrt{\frac{k_2}{\beta}} \operatorname{Tan}^{-1}\sqrt{\frac{\beta}{2}}\right) \frac{H_b^{1/2}}{g^{1/2} \operatorname{Tan} \alpha} \tag{6}$$

and

$$t_d = 2\sqrt{\frac{k_2}{\beta}}\exp\left(\frac{\beta}{4}\frac{k_3 + \frac{1}{k}}{k_2}\right)\frac{H_b^{1/2}}{g^{1/2}\,\mathrm{Tan}\,\alpha} \tag{7}$$

where

$$\beta = \frac{fV_0^2}{4t_h \sin\alpha}$$

and k_3 is a runup coefficient as shown in Fig. 2.

Based upon Eqs. (3), (6), and (7), the swash period of a single wave can be determined:

$$T_n = K\frac{H_b^{1/2}}{g^{1/2}\,\mathrm{Tan}\,\alpha} \tag{8}$$

where

$$K = K_1 + K_2 + K_3$$

with

$$K_1 = \frac{\sqrt{2}(\sqrt{k_2} - \sqrt{k_1})}{k(k_2 - k_1)}$$

$$K_2 = 2\sqrt{\frac{k_2}{\beta}}\,\mathrm{Tan}^{-1}\sqrt{\frac{\beta}{2}}$$

$$K_3 = 2\sqrt{\frac{k_2}{\beta}}\,\mathrm{Exp}\left(\frac{\beta}{4}\frac{k_3 + \frac{1}{k}}{k_2}\right)$$

Therefore, the natural swash period is found to be a function of $\frac{H_b^{1/2}}{g^{1/2}\,\mathrm{Tan}\,\alpha}$. We now define a non-dimensional surf zone parameter as the ratio of natural swash period to the incoming wave period (T):

$$I_w = \frac{T_n}{KT} = \frac{H_b^{1/2}}{g^{1/2}T\,\mathrm{Tan}\,\alpha} \tag{9}$$

This non-dimensional parameter has the same form as the one suggested by Iribareu and Nogales (1949) to define breaking criterion. Battjes (1974), through dimensional reasoning, came to a similar non-dimensional parameter, which he amplified its significance to a variety of surf zone phenomena, including breaking type classification, set-up and set-down, etc. In here, we add another physical implication which can be explained as follows:

The I_w is the surf zone interference index. When I_w is small, each individual wave will complete the swash cycle with little or no interference from the successive waves. The flow in the swash zone is mainly oscillating and the breaker is of the plunging type. When I_w increases, the degree of interference from successive waves also increases; a circulatory motion is gradually developing which will result in a return flow in the main water column; the breaking phenomenon gradually transforms from plunging to spilling. This sequence of events is illustrated in Fig. 3.

This surf parameter also seems to play an important role in the similarity model to be presented in the following sections.

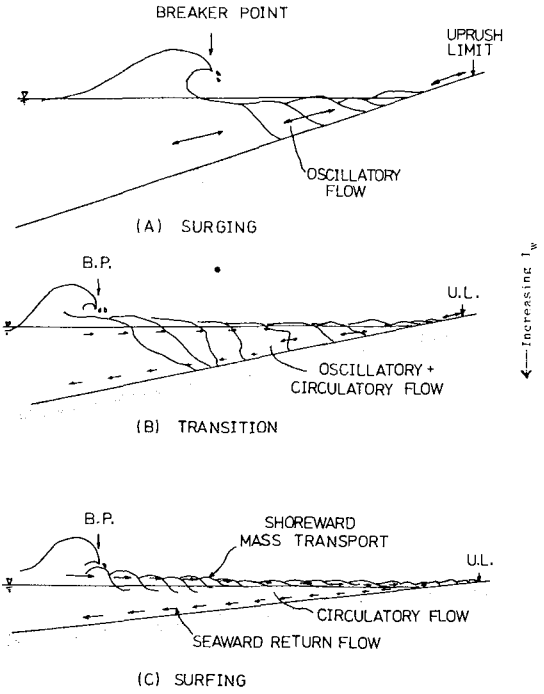

FIGURE 3. BREAKER CLASSIFICATION BASED UPON I_w.

3. BREAKING WAVE SIMILARITY

For a wave train of single frequency shoaling on a beach, a more or less amount of energy is being transferred from the primary wave component to its higher harmonics. The amplitude dispersing among harmonics coupled with phase lags developed due to differential shoaling of each harmonic component results in a highly asymmetric wave form upon breaking.

After breaking, as the wave travels further inshore, the wave form tends to stabilize although it remains asymmetrical. The conventional higher order wave theories are no longer adequate to describe these asymmetrical wave forms. A variation would be the introduction of phase angles among harmonic components such that the water surface fluctuation is expressed as

$$\eta(t) = \sum_{n=1}^{\infty} a_n \sin(n\sigma t + \phi_n') \tag{10}$$

where a_n is the nth harmonic amplitude; ϕ_n' is the nth harmonic phase and σ is the fundamental frequency.

Equation (10) most certainly can be used to prescribe the wave form of any particular set of breaking waves. Yet, it serves little useful engineering purpose if the solution cannot be generalized. If we assume that (1) each harmonic amplitude is limited by the local water depth, and (2) the phase velocity of each harmonic is also depth limited, then, we have

$$a_n = \alpha_n(d + \bar{\eta}) \tag{11}$$

and

$$C_n \alpha \sqrt{g(d + \bar{\eta})} \tag{12}$$

where $\bar{\eta}$ is wave setup. Equation (10) can now be expressed as:

$$\frac{\eta(t)}{d + \bar{\eta}} = \sum_{n=1}^{\infty} \alpha_n \sin(n\sigma t + \phi_n) \tag{13}$$

where α_n's are non-dimensional coefficients and ϕ_n's are constant phase angles. Thus, the wave profile remains similar and its magnitude is affected only by a local parameter $(d + \bar{\eta})$.

In shallow water, if we express the depth averaged horizontal velocity in terms of η, we have

$$u(t) = \frac{C\eta(t)}{d} + \text{higher order terms of } \eta \tag{14}$$

recognizing that the net contribution of the higher order terms is a

mean return flow in the water column, Eq. (14) becomes

$$u(t) = \frac{C\eta(t)}{d} - \bar{U}_R \tag{15}$$

The fact of having a similarity solution of $\eta(t)$, leads to the following similarity solutions for $u(t)$:

$$\frac{u(t) + \bar{U}_R}{C(1 + \frac{\bar{\eta}}{d})} = \sum_{n=1}^{\infty} \beta_n \sin(n\sigma t + \psi_n) \tag{16}$$

where β_n and ψ_n are constant coefficients.

Since C can be approximated by

$$C = \kappa\sqrt{g(d + \bar{\eta})} \tag{17}$$

we have

$$\frac{u(t) + \bar{U}_R}{\kappa\sqrt{g(d + \bar{\eta})}(1 + \frac{\bar{\eta}}{d})} = \sum_{n=1}^{\infty} \beta_n \sin(n\sigma t + \psi_n) \tag{18}$$

The solution $u(t)$ now depends only upon certain local parameters d, $\bar{\eta}$ and $\bar{U}_R$.

4. LABORATORY EXPERIMENT

To check the validity of the similarity solutions, experiments were conducted in a wave tank shown in Fig. 4. Water surface variations and horizontal particle motions were measured at four stations inside the surf zone on a smooth beach with a slope m = 0.1. The waves were measured by motion pictures and the horizontal particle velocity was measured by an air bubble system following the same principle as the hydrogen bubble system for flow visualization (for detailed measurement techniques see Yang, 1980). Since the wave flow field is unsteady, the dynamic response of an air bubble is established as shown in Fig. 5.

A total of ten sets of experiments were conducted. The test conditions are summarized in Table 1.

5. RESULTS

The wave amplitude coefficients, α_n, and wave phase coefficients, ϕ_n, of the first five harmonics are shown in Fig. 6 plotted against the surf parameter, I_w. The phase angles are adjusted so that $\phi_1 = 0$. These data are quite scattered but the trend is clear. Both α and ϕ become constant when I_w becomes large. Since a large I_w corresponds to a spilling breaker, the results seem to indicate a similarity solution,

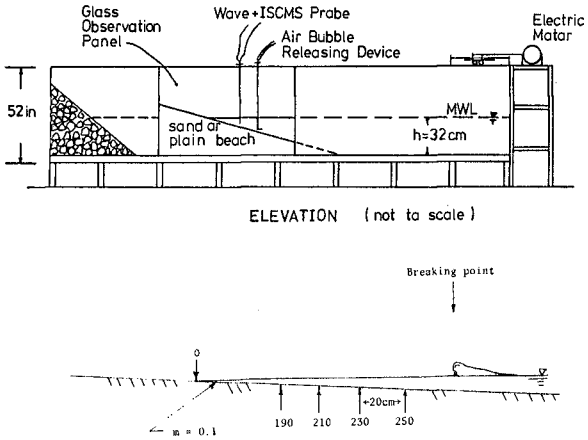

FIGURE 4, LABORATORY SETUP.

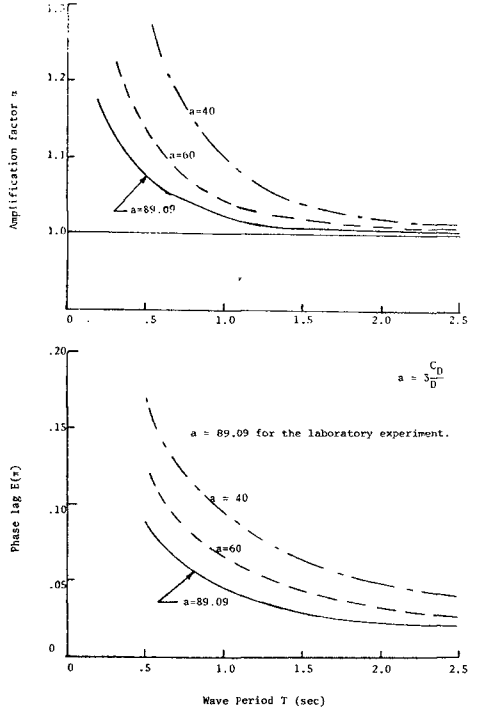

FIGURE 5, DYNAMIC RESPONSE OF AIR BUBBLE IN THE WAVE FIELD.

TABLE 1. EXPERIMENTAL CONDITIONS

Run No.	Incident Wave Height H_c (cm)	Breaking Wave Height H_b (cm)	Wave Period T (sec)	$\frac{H_b^{1/2}}{g^{1/2}TM}$
LAB CONDITIONS (DELAWARE)				
PB-1	9.5	11.5	2.0	.54
PB-2	11.0	14.0	1.8	.66
PB-3	11.0	14.0	1.6	.75
PB-4	13.5	14.0	1.4	.85
PB-5	10.0	11.5	1.2	.90
PB-6	11.0	12.5	1.0	1.13
PB-7	10.5	11.5	1.0	1.08
PB-8	9.0	10.0	1.0	1.01
PB-9	8.0	9.0	1.0	.96
PB-10	6.0	7.5	1.0	.88
LAB CONDITIONS (ISVA) (1978)				
070703		4.12	1.43	1.50
070705		4.43	1.43	1.64
451015		5.25	2.22	1.12
451018		4.95	2.22	1.09
LAB CONDITIONS (SAKAI AND IWAGAKI) (1978)				
2-2-2		9.4	1.24	1.58
3-2-1		11.5	1.24	2.27

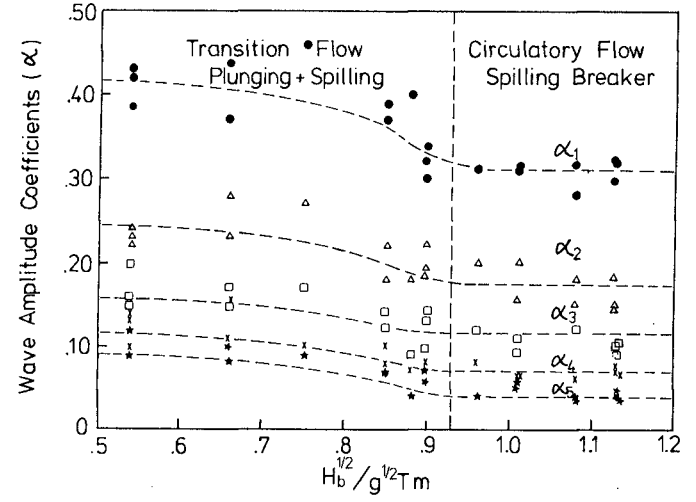

a)

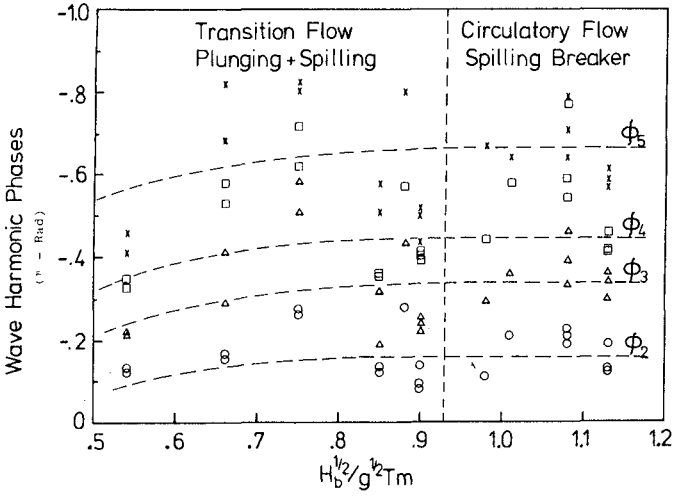

b)

FIGURE 6. WAVE AMPLITUDE COEFFICIENTS AND PHASE COEFFICIENTS VS. I_w.

if exists, would be in the spilling breaker region where I_w is larger than 0.9. In the case of horizontal velocity, the amplitude and coefficients are plotted against I_w as shown in Fig. 7. These data reveal that the similarity solution also yields reasonable approximations for large I_w. In fact, the similarity approximations for velocity seems to extend to regions of smaller I_w than the corresponding region where the similarity solution of η becomes valid, i.e. velocity profile approaches similar form as early as the transition flow zone, whereas the surface profile will not become similar until spilling breaker condition is attained.

Figure 8 plots the non-dimensional surface variation for various experiments. In there, data from Svendsen et al. (ISVA, 1978) and Sakai and Iwagaki (1978) are also shown. Both Svendsen's and Sakai's data are well within the spilling breaker region (I_w ranging from 1.12 to 2.27). Their test conditions are listed in Table 1. All the data sets seem to exhibit a gross similarity feature. A closer examination of these profiles reveals that the fine features of similarity vary for data sets obtained by different investigators. These variations can best be explained with the aid of Table 2 where the statistics of the coefficients in the similarity solution are tabulated. First of all, the standard deviations of the amplitude coefficients are all very small (no more than 4% from the mean), which means the similarity solution is good in the region specified. On the other hand, the absolute value of α's are different. The present laboratory value data and Sakai and Iwagaki's values are very close. They both differ somewhat from ISVA's values. The relative importance of each harmonic component can be assessed from the values listed under $\alpha/\Sigma\alpha$. For instance, the fundamental component has a value of 0.4 to 0.5. The total contribution due to harmonics higher than third is usually less than 20%. In terms of wave height, the effect of these higher harmonics is insignificant because of the phase shift. In terms of energy, their contributions are even less. The relative importance of the first three harmonic components is quite consistent among the three sets of data. The results of phase angle are somewhat unexpected. All the data show that the second harmonic leads the first harmonic and the third harmonic leads both first and second. One would expect the other way around as the higher harmonics should have smaller phase velocities. The values of phase coefficients are very close for the Delaware and ISVA data. They both differ from Sakai and Iwagaki's value. This point is further examined later.

Figure 9 illustrates the non-dimensional velocity profiles. The statistics of velocity harmonics are also tabulated in Table 2. In here, the fundamental component dominates the others. The higher component lags the successive lower component as expected. However, these phase lags are all very small. The combined effects of dominant fundamental components and small phase shift result in a more symmetrical profile than that of wave forms. The same kind of results have been obtained by Flick (1978) and Thornton (1976). A tentative explanation has been offered on the reasoning that bottom and internal frictions tend to dampen the higher wave components at a fast rate. The experimental data also show here that the peak horizontal velocity always lags the peak water surface variation such as illustrated by an example in Fig. 10.

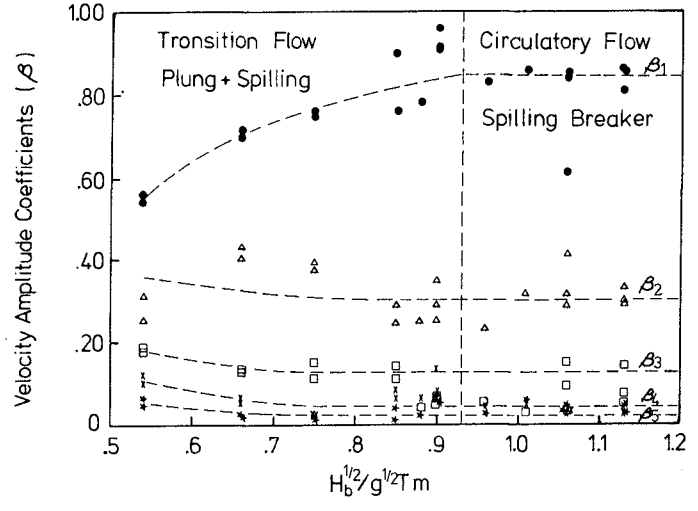

a)

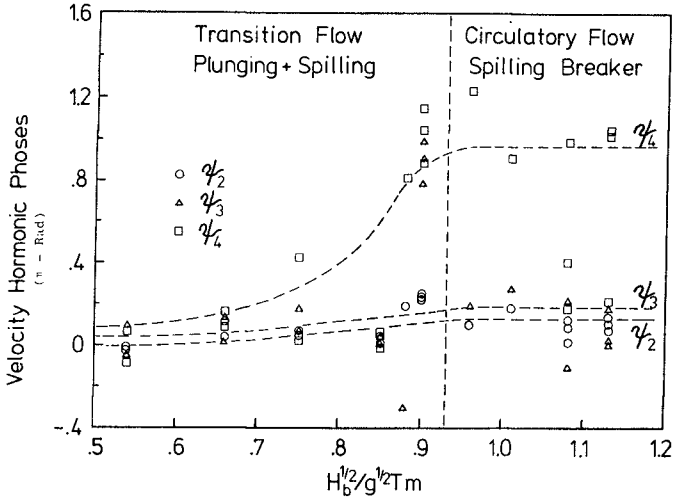

b)

FIGURE 7, VELOCITY AMPLITUDE COEFFICIENTS AND PHASE COEFFICIENTS VS. I_w.

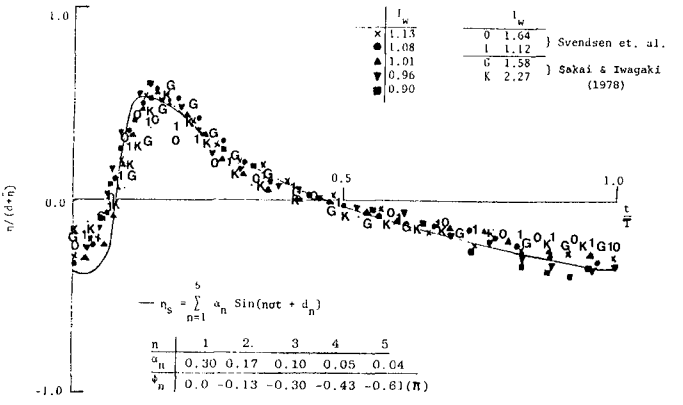

FIGURE 8. NON-DIMENSIONAL SURFACE PROFILES.

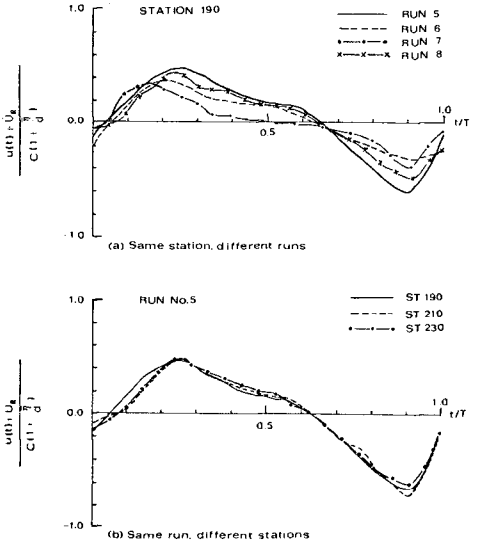

FIGURE 9. NON-DIMENSIONAL VELOCITY PROFILES.

TABLE 2. STATISTICS OF AMPLITUDE COEFFICIENTS AND PHASE COEFFICIENTS.

AMPLITUDE HARMONICS

Source	Amplitude (α)				Phase (ϕ)			No. Exps.
		Mean	σ	$\alpha/\Sigma\alpha$		Mean	σ	
Delaware	α_1	0.30	0.038	0.41	ϕ_1	--	--	9
	α_2	0.17	0.022	0.22	ϕ_2	-0.13π	0.027	
	α_3	0.10	0.011	0.15	ϕ_3	-0.30π	0.22	
ISVA	α_1	0.23	0.035	0.47	ϕ_1	--	--	32
	α_2	0.11	0.016	0.22	ϕ_2	-0.14π	0.08	
	α_3	0.07	0.012	0.14	ϕ_3	-0.28π	0.14	
Sakai and Iwagaki	α_1	0.32	--	0.48	ϕ_1	--	--	2
	α_2	0.15	--	0.23	ϕ_2	-0.25π	--	
	α_3	0.09	--	0.13	ϕ_3	-0.40π	--	

VELOCITY HARMONICS

Source	Amplitude (β)				Phase (ψ)			No. Exps.
		Mean	σ	$\beta/\Sigma\beta$		Mean	σ	
Delaware	β_1	0.81	0.078	0.63	ψ_1	--	--	8
	β_2	0.30	0.054	0.23	ψ_2	0.05π	0.09	
	β_3	0.08	0.043	0.06	ψ_3	0.07π	0.15	

σ: standard deviation

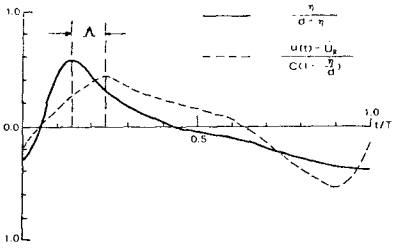

FIGURE 10. COMPARISONS OF SURFACE AND VELOCITY PROFILE.

As the wave breaks on a slope, the motion appears to be quite disorderly. When the breaking wave proceeds up-slope, it gradually regains its regular appearance. The question is how far shoreward from the breaking point beyond which the similarity solution can be considered adequate. For this purpose, the phase angles are plotted against the non-dimensional depth d/d_b and d_b the depth at the breaking point. Four sets of data from different investigators are shown in Fig. 11. In here, the phase coefficients are defined in terms of cosine phase lag, i.e.,

$$\eta = \sum_{n=1}^{\infty} \alpha_n \cos(n\sigma t + \zeta_n) \tag{19}$$

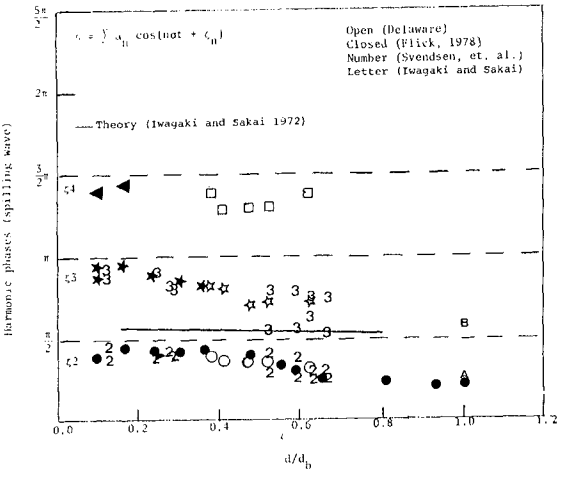

FIGURE 11. VARIATIONS OF PHASE COEFFICIENTS AS A FUNCTION OF d/d_b.

The relationship between ζ_n and ϕ_n, which is defined as the sine phase lag, is

$$\zeta_n = (n - 1)\frac{\pi}{2} + \phi_n \tag{20}$$

These phase coefficients are shown to vary slowly with d/d_b and approach limits at $\pi/2$ intervals when $d/d_b \to 0$. Since the profiles measured by Sakai and Iwagaki are near the breaking point, the results in this figure explain why they differ from that of the present experiment and that of ISVA; both were carried out in the inner zone where $d/d_b < 0.7$.

To utilize the similarity equations to describe the breaking wave properties one must have knowledge of $\overline{U}_R$ and κ as appeared in Eq. (18). At present, we are unable to predict either. The experimental results of these quantities are, however, shown in Figs. 12 and 13 respectively. It appears that the return flow strength increases with increasing I_w but gradually reaches a constant in the spilling breaking region. The κ value, on the other hand, decreases with increasing I_w. Since κ is actually the ratio of wave celerity and $\sqrt{gd}$, the results are the consequence that spilling breakers travel slower than plunging breakers.

6. CONCLUSIONS

Assuming both the water surface variations and the depth-averaged horizontal particle velocities in the surf zone can be expressed by the summation of Fourier components, similarity solutions are proposed here. These solutions are based upon a pair of rather restrictive conditions; namely, both the amplitude and the phase velocity of each harmonic component are depth limited. The solutions, however, offer the advantage of being simple and completely defined by a few local flow parameters.

Laboratory data from a number of investigators including those obtained by the authors are used to test the validity of the proposed solutions.

The results seem to suggest that the similarity solution is not universally applicable. However, if the wave is of the spilling type and is far inshore in the inner breaking zone, the similarity solution becomes suitable to describe the mean flow characteristics. These conditions can be defined in terms of a surf parameter $I_w = \frac{H^{1/2}}{g^{1/2} T \tan \alpha}$ and a relative depth parameter d/d_b. The region of suitability is found to be when $I_w > 0.9$ and $d/d_b < 0.6$. In this region, both surface profile and horizontal velocity can be adequately described by the first three harmonics. The velocity profile is found to be less asymmetric than the surface profile.

For surface profile, the higher harmonics lead the lower ones whereas the contrary is true for the velocity profile.

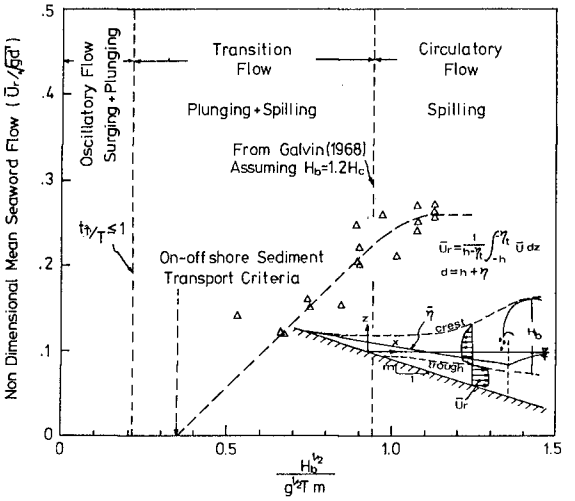

FIGURE 12. RETURN FLOW VS. I_w.

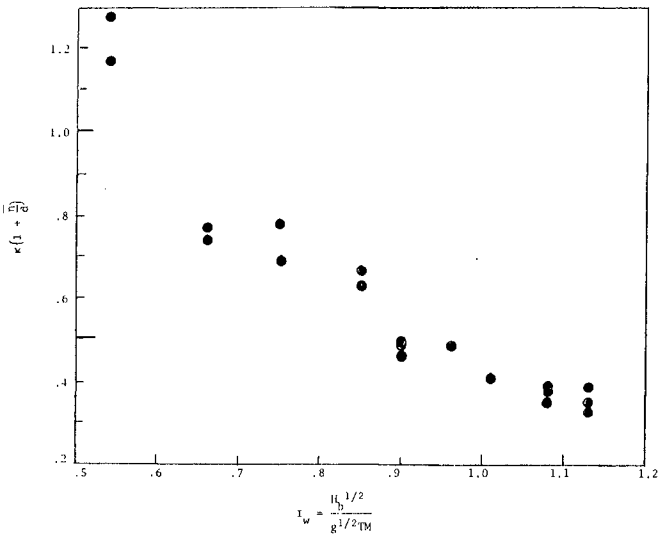

FIGURE 13. κ VS. I_w.

7. ACKNOWLEDGMENT

The work is supported by the Office of Naval Research Geography Branch under Contract No. N00014-76-C-0342. The authors wish to thank Dr. I. A. Svendsen of the Institute of Hydrodynamics and Hydraulic Engineering, Technical University of Denmark, who provided their laboratory data.

8. REFERENCES

Battjes, J. A. (1974), "Surf Similarity", Proc. 14th Coastal Engineering Conference, Copenhagen, Denmark, p. 466-479.

Flick, R. F. (1978), "Study of Shoaling Waves in the Laboratory", Ph.D. Dissertation, University of California, San Diego, pp. 159.

Iribarren, C. R. and Nogales, C. (1949), "Protection Des Ports", Section II, Comm. 4, XVIIth Nav. Congress, Lisbon, p. 31-80.

Sakai, T. and Iwagaki, Y. (1978), "Estimation of Water Particle Velocity of Breaking Wave", Proc. 16th Coastal Engineering Conference, Hamburg, Germany, p. 551-568.

Svendsen, I. A., Madsen, P. A., and Hansen, J. B. (1978), "Wave Characteristics in the Surf Zone", Proc. 16th Coastal Engineering Conference, Hamburg, Germany, p. 520-539.

Thornton, E. B. et al. (1976), "Kinematics of Breaking Waves", Proc. 15th Coastal Engineering Conference, Hawaii, Vol. I, p. 461-476.

Yang, W. C. (1980), "Surf Zone Properties and Onshore-Offshore Sediment Transport", Ph.D. Dissertation, Dept. of Civil Engineering, University of Delaware (in preparation).